July 6, 2012

Hiroyuki Noumi
RCNP, Osaka University
for the E31 collaboration

To the FIFC(PAC) chairperson and members:

I am writing to report the preparation status for the E31 experiment, "Spectroscopic study of hyperon resonances below $\bar{K}N$ threshold via the (K^-,n) reaction on Deuteron". In this report, we demonstrate readiness for experiment and request a stage-2 approval.

The E31 experiment is aiming to clarify whether $\Lambda(1405)$ is a $\bar{K}N$ resonant state as predicted by the chiral unitary model or not. To accomplish this aim, we will measure the $\Lambda(1405)$ state via the (K^-,n) reaction to test whether the resonance appears at ~1420 MeV/c^2 as predicted by the chiral unitary model [1] or at ~1405 MeV/c^2 as deduced by Dalitz *et al.* [2]. This experiment will provide vital and most fundamental information on the longstanding argument of the deeply bound kaonic nuclear state. Although we do not repeat detailed explanation of E31 here, we attached an updated proposal with an addendum.

Experimental setup for E31 is almost the same as that for E15 (Fig. 1). Backward proton detectors and a deuteron target are additionally prepared for E31 (Fig. 2). Construction for the E15 setup was finished recently, and commissioning run for E15 has been successfully completed very recently. Readiness of E15 for physics run will be presented in the coming PAC. A negative kaon beam tuning was successfully done at 1.0 GeV/c. It is confirmed that a kaon intensity of 10^4 per pulse per 1kW primary proton beam can be obtained with keeping a kaon/pion ratio of as good as 0.3. This intensity corresponds to 3×10^5 kaons per pulse at a primary beam power of 27 kW assumed in the proposal, which is 1.5 times higher than we expected, thanks to the 6 cm thick Pt target used for the primary target.

Backward proton detector system is necessary to identify an important decay mode of $\Lambda(1405) \rightarrow \Sigma^0\pi^0$. The system comprises plastic scintillation counter hodoscopes (BPD) and a multi-wire drift chamber (BPC). BPD is used to measure a time of flight of a particle from the produced hyperon state. It has been installed in a narrow space between the end-cap yoke of the CDS solenoid magnet and the endplate of the

cylindrical drift chamber (CDC), located about 50 cm upstream from a center of the cylindrical detector system (CDS). It covers 350mmx340mm area with 70 slabs of a plastic scintillator of 5mm x 5mm x 340mm (Fig. 3). Because of a strong magnetic field and a narrow space at BPD, we employ Multi-Pixel Photon Counters (MPPC) of 3mm x 3mm sensing area for photon sensors. In the proposal, we assumed a resolution of a time of flight (TOF) between BPD and T0 to be 200 ps in order to identify the $\Lambda(1405) \rightarrow \Sigma^0\pi^0$ decay mode from other modes, such as $\Sigma(1385) \rightarrow \Lambda\pi^0$. Here, T0 is a time zero counter installed about 50 cm downstream of BPD. In the recent commissioning run, we demonstrated the TOF resolutions of about 130 ~ 190 ps, as shown in Fig. 4. Fig. 5 shows a correlation between the TOF and pulse height of a BPD segment measured for the pion and proton beam at 1 GeV/*c*. Protons are clearly separated from pions.

BPC is placed just upstream the target. It has a cylindrical, gas-tight volume of 168 mm in diameter and 90mm in length (Fig. 6-left). Eight sense wire planes of XX'YY'XX'YY' are installed inside this volume. Each plane has a disk shape of sensitive area of 111.6mm in diameter (Fig. 6-right). Sense wires and potential wires are alternately placed in an interval of 3.6 mm. In XX' (YY'), wire positions are 3.6 mm staggered each other. Ar and Isobutan gases mixed with a ratio of 80:20 are used. BPC has already been installed and operated in CDS. BPC shows a good performance; measured residual distribution for tracked events is found to be 90~110 μm in sigma, as shown in Fig. 7. Fig. 8 (left) shows a clear image of the target cell reconstructed from BPC.

We developed a deuterium target system. The target configuration, as shown in Fig. 9, is similar to that of ^{3}He for E15. In E31, a G-M refrigerator is employed to liquefy the deuterium at the heat exchanger. We control the temperature of liquid deuterium by controlling a heater attached nearby the cold finger. We successfully demonstrated to liquefy the hydrogen and keep its temperature at 20K within a fluctuation level of 0.2K, as shown in Fig. 10. We find that the cooling power is still kept at 13 W. This temperature fluctuation causes a density fluctuation at a level of 0.3%. The deuterium is solidified below 18.7 K. If the solid deuterium is made in the transfer pipe, the thermal stability is lost at the target cell. As the worst result, the deuterium gas explosively blows up to break down the target system. Therefore, this level of stability is necessary to avoid solidification. A buffer tank with a safety valve will be connected for further safety. The deuteron target system will be reviewed by the safety committee.

We have finished hardware preparation for the E31 experiment. We expect to start experiment within a several days to switch the target system after the E15 first stage

run finishes. Then, it would be worthy to mention about milestones for E31. We stress an advantage of the d(K^-,n) reaction that enhances S-wave $\bar{K}N$ scattering to form $\Lambda(1405)$. We wish to confirm first if this characteristic reaction mechanism is realized. To do it, we do not think to spend much time. In the first 10 kW*week run or so, we expect to collect more than 1000 events of the $\Lambda(1405)$–>$\Sigma^-\pi^+$ decay modes, which exceeds more than twice the number of events of existing data in the d(K^-,n)$\Sigma^-\pi^+$ reaction [3]. In the same time, we expect to observe the $\Sigma^+\pi^-$ decay mode in the d(K^-,n) reaction for the first time at a level of more than a few hundred events in statistics. We can accumulate data of $\Sigma^-(1385)$ production via the d(K^-,p) reaction simultaneously. Comparison of the d(K^-,p) spectrum with the d(K^-,n) one, *i.e.* difference of the line shapes and the cross sections, would enhance a validity of the discussion. It is interesting to discuss difference of the formation cross sections in terms of the structures of the two resonant states. In these respects, we prefer to start data taking at the earliest opportunity.

References:

[1] D. Jido, E. Oset, and T. Sekihara, "Kaonic production of $\Lambda(1405)$ off deuteron target in chiral dynamics", Eur.Phys.J.A42:257-268,2009.

[2] R. H. Dalitz and A. Deloff, J. Phys. G17, 289(1991).

[3] O. Braun *et al.*, Nucl. Phys. B129, 1(1977).

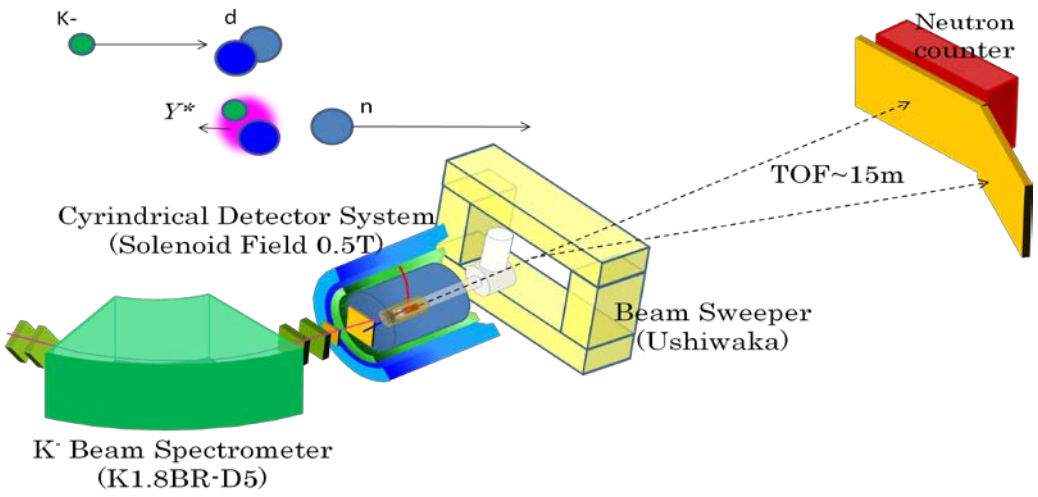

Fig. 1: Schematic layout of the E31 setup. A kaon beam at 1 GeV/c is irradiated on the deuteron target. A neutron is kicked at the forward angle to form Λ(1405).

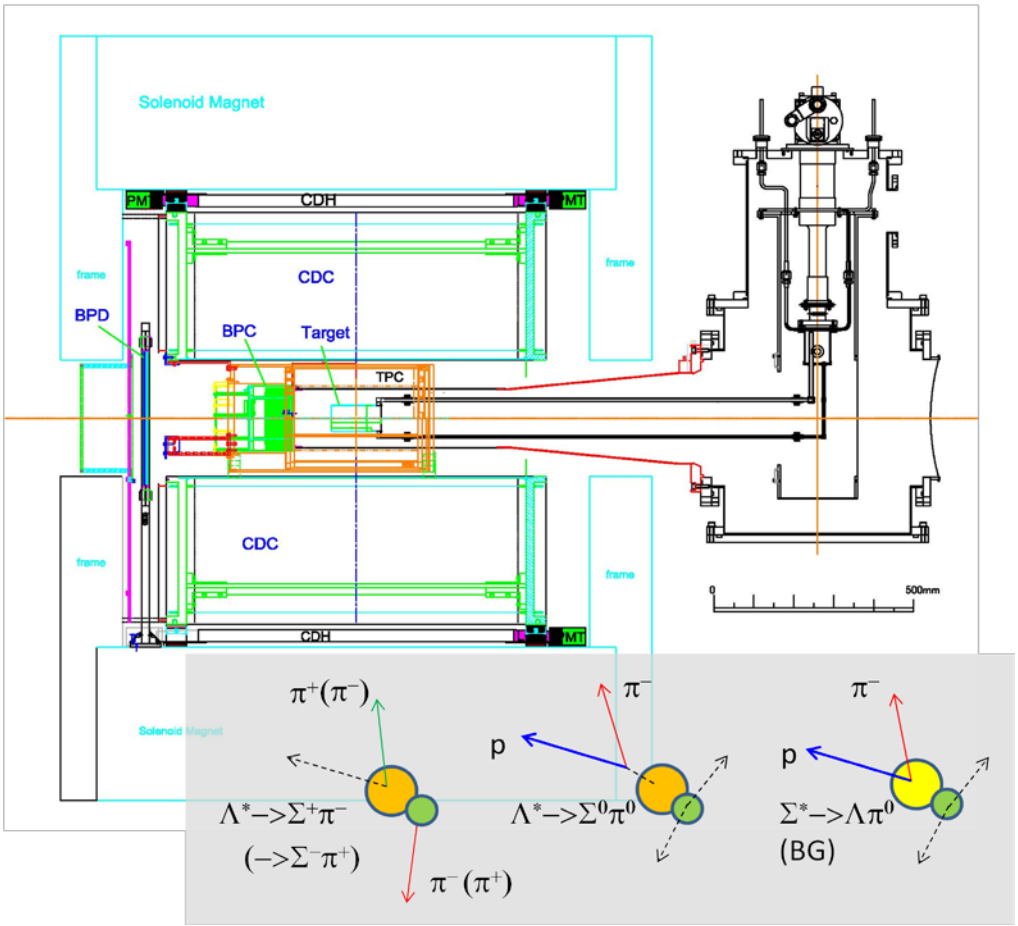

Fig. 2: Side view of the Cylindrical Detector System and the deuteron target. BPD and BPC are installed to detect backward emitted proton. Typical decay topologies from produced hyperon resonances are also shown.

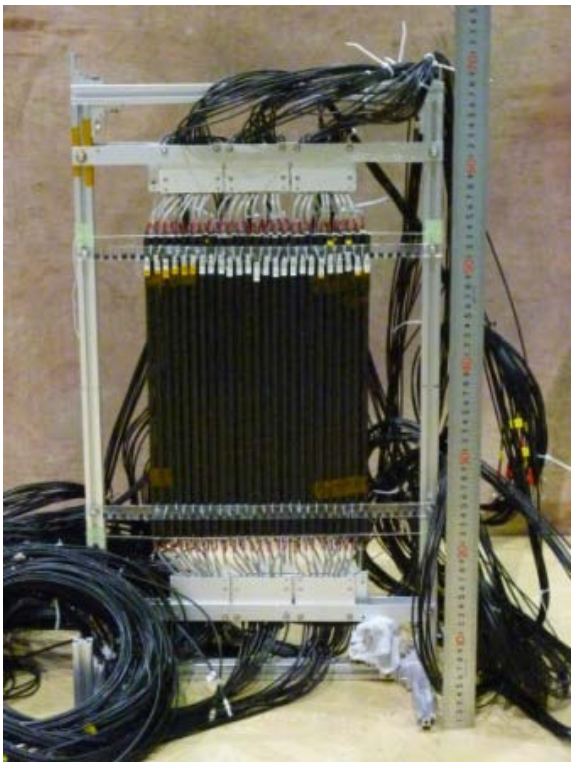

Fig. 3: Photograph of BPD.

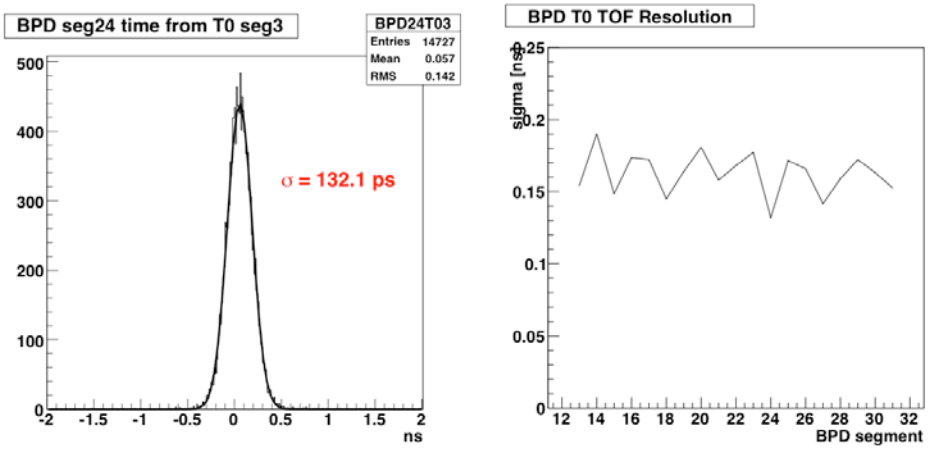

Fig. 4: (Left) Time of flight is measured between BPD (BPD#24) and T0 segment #3. It is fit by a Gaussian function with the sigma of 132 ps. (Right) Time-of-flight resolutions measured between other segments of BPD and T0 segment #3 for the 1-GeV/c pion beam at K1.8BR are shown.

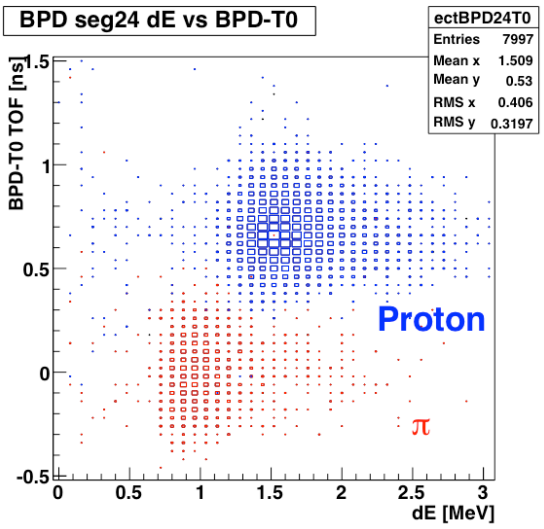

Fig. 5: Two dimensional plot of the TOF between BPD and T0 versus energy deposit at BPD measured for pion and proton beams at 1 GeV/*c*.

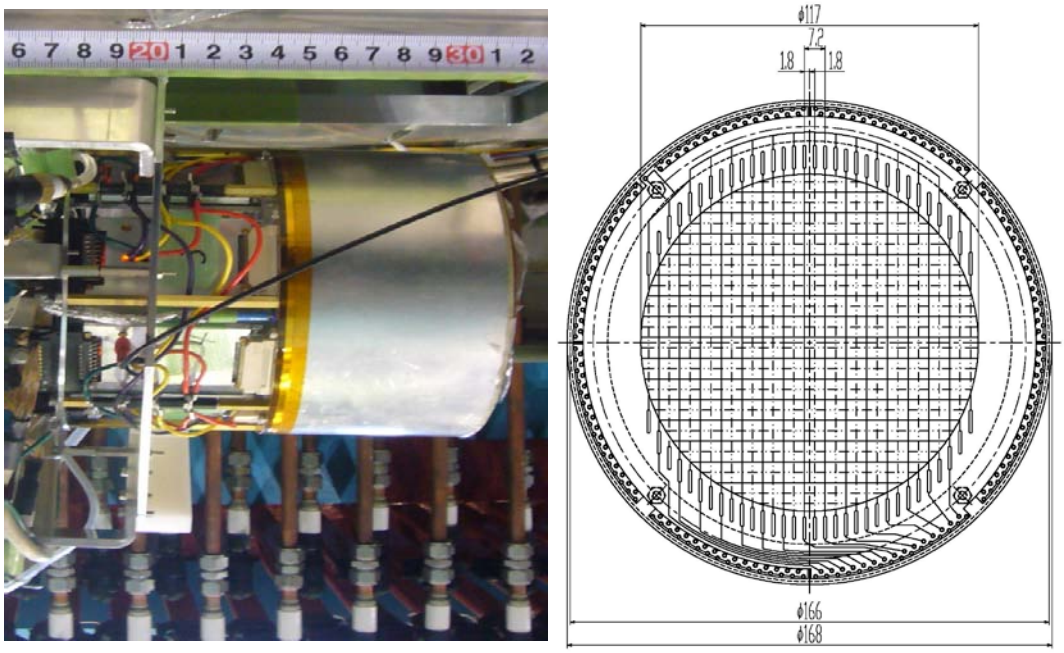

Fig. 6 : Photograph of BPC (Left) and Drawings of a wire plane (Right). 17 potential and 15 anode wires are placed alternately in an interval of 3.6 mm. Mirror configuration planes are prepared to solve so-called left-right ambiguity.

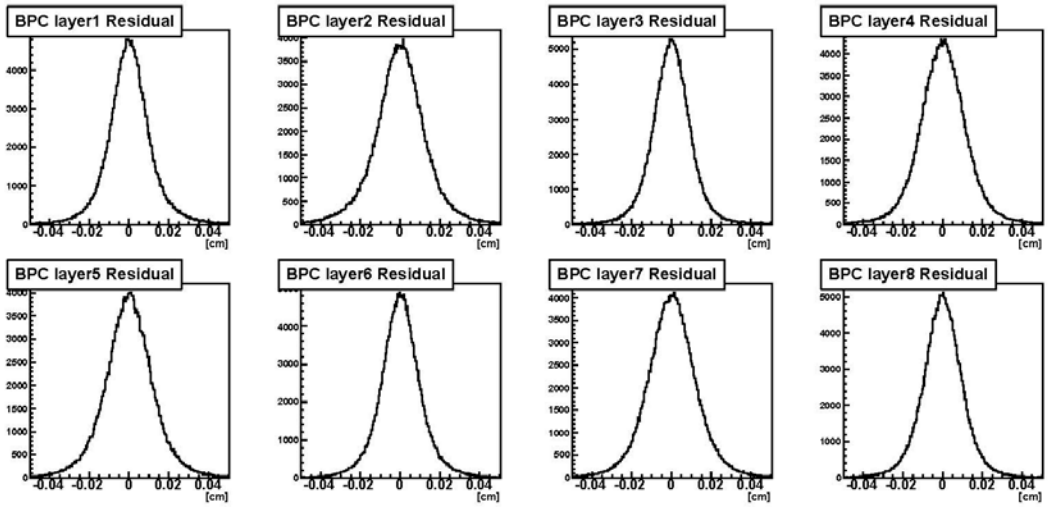

Fig. 7: Residual distributions for reconstructed tracks by BPC. The widths are found to be 90 ~ 110 μm in 1 sigma. Layers 1 to 8 stand for XX'YY'XX'YY' planes. Layer 1 is located upstream.

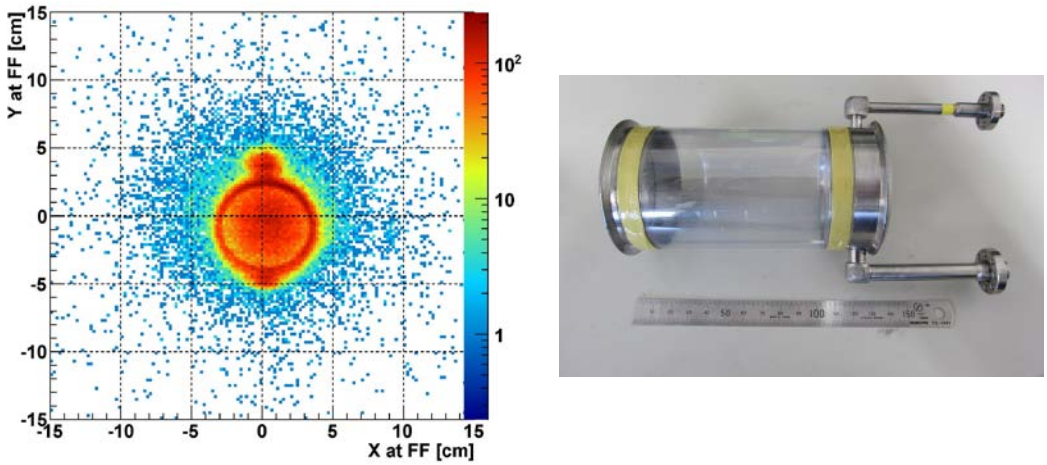

Fig. 8: (Left) A target image seen on the beam is clearly reconstructed by BPC for the events that require two CDH hits in the trigger. Image of the liquid target (^{4}He in this case) can be seen at around the center position together with a ring image of the target cell. (Right) A target cell used is shown here. The beam is coming from left hand side.

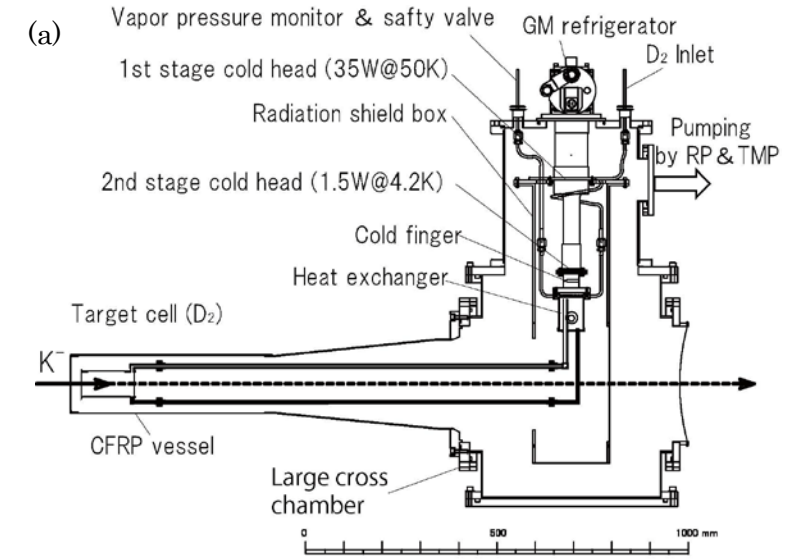

Fig. 9: (a) Drawings of the deuteron target system (side view). A double-stage G-M refrigerator is used to liquefy the deuterium at the heat exchanger. Liquid deuteron is filled in the target cell through a long transfer tube. (b) A photograph of the target cell connected with the heat exchanger via transfer tubes. The cell is surrounded by super insulator films as a radiative heat load protection. (c) A photograph of the target system.

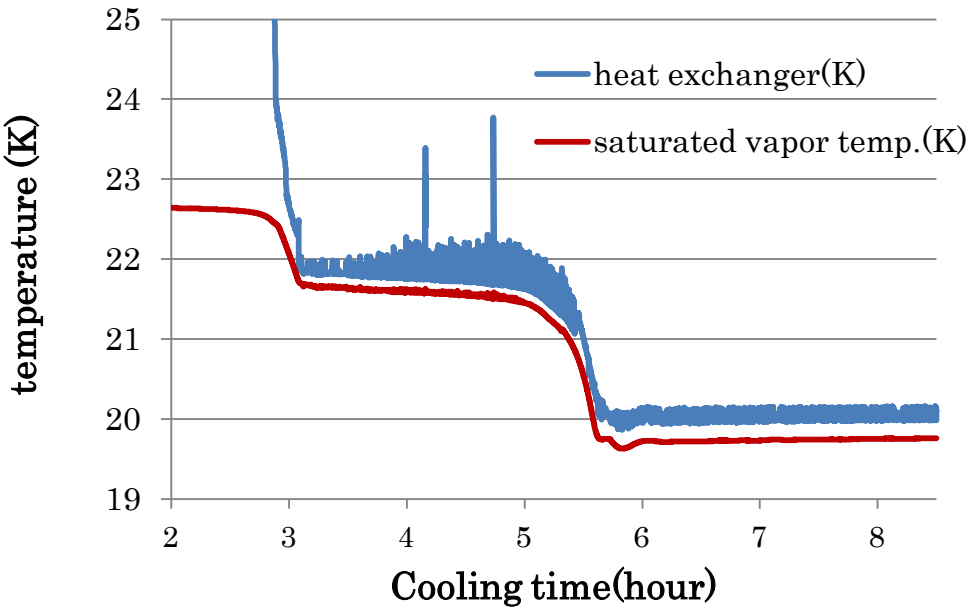

Fig. 10: Time development of the target temperature in the cooling test with hydrogen at KEK. The heater current is controlled so that the temperature at the heat exchanger is kept at 20 K. Spikes appear in the blue line are regarded as electric noises. The temperature of liquid hydrogen pooled in the target cell is evaluated from measured vapor pressure, as shown in the brawn line.